Fatigue strength assessment of TIG-dressed ultra-high-strength steel fillet weld joints using the 4R method

Mettänen Heli, Nykänen Timo, Skriko Tuomas, Ahola Antti, Björk Timo

DOI: 10.1016/j.ijfatigue.2020.105745

Fatigue strength assessment of TIG-dressed ultra-high-strength steel fillet weld joints using the 4R method

H. METTÄNEN[1], T. NYKÄNEN[1], T. SKRIKO[2], A. AHOLA[1], T. BJÖRK[1]

[1]*Laboratory of Steel Structures, School of Energy Systems, Lappeenranta-Lahti University of Technology LUT, P.O. Box 20, FIN-53851 Lappeenranta, Finland*
[2]*Laboratory of Welding Technology, School of Energy Systems, Lappeenranta-Lahti University of Technology LUT, P.O. Box 20, FIN-53851 Lappeenranta, Finland*

ABSTRACT

Post-weld treatments can enhance the fatigue strength of weldments by means of improving their geometry or residual stresses, or both. In this study, the fatigue strength of TIG-dressed non-load-carrying cruciform joints made of ultra-high-strength steel were analyzed using stress-based approaches, i.e. nominal, structural, and effective notch stress (ENS) methods, and a multi-parametric approach, entitled the 4R method. Comparisons were made between the methods, along with the applied parameters, and the results showed the 4R and ENS approaches to have the best correspondence with the experimental test data, whereas the nominal and structural stress methods resulted in conservative fatigue strength estimations.

Keywords: Welded joints; fatigue; 4R method; ultra-high-strength steel; TIG-dressing.

NOMENCLATURE

ASW	as-welded condition
CA	constant amplitude
ENS	effective notch stress
FAT	fatigue class, fatigue strength corresponding to two million cycles
HAZ	heat affected zone
IIW	International Institute of Welding
MSSPD	minimization of the sum of squared perpendicular distances
SCF	stress concentration factor
SWT	Smith-Watson-Topper
TIG	tungsten inert gas
UHSS	ultra-high-strength steel

A	elongation
C	fatigue capacity
d	undercut
E	Young's modulus
f_y	yield strength
H	cyclic strain hardening coefficient
K_f	fatigue notch factor
K_s	structural stress concentration factors
$K_{t,m}$	elastic stress concentration factor for axial load
$K_{t,b}$	elastic stress concentration factor for bending load

Correspondence : H. Mettänen. Tel: +358 445039366, E-mail: heli.mettanen@lut.fi

m	slope of the stress-life curve in a log-log graph
N_f	cycles to failure
n	cyclic strain hardening exponent
R	stress ratio
R_m	ultimate strength
$R_{p0.2}$	yield strength
r	weld toe radius
T_σ	scatter range
t	plate thickness
y	weld profile parameter
α	angular misalignment
Δ	range
ε	total strain
ε_e	elastic strain
ε_p	plastic strain
σ	stress
σ_k	effective notch stress

Indices

b	bending
char	characteristic value corresponding to 95 % survival probability
HS	hot spot
local	local value
m	mean value, membrane
max	maximum value
mean	mean value corresponding to 50 % survival probability
min	minimum value
nom	nominal value
ref	reference value
res	residual stress
s	structural
true	measured value

INTRODUCTION

The fatigue life of a welded joint is usually calculated using conventional stress-based methods, i.e. the nominal stress, structural hot spot stress, and effective notch stress (ENS) methods, and current guidelines and design codes [1,2] recommend these methods. However, the above-mentioned methods do not consider all the factors that can have a significant effect on fatigue strength, including material ultimate strength ($\boldsymbol{R}_m$), quality of the weld toe in terms of the toe radius ($\boldsymbol{r}_{\text{true}}$), residual stress ($\sigma_{\mathbf{r}\text{es}}$), and the applied stress ratio ($\boldsymbol{R}$). In this research work, the fatigue strength of TIG-dressed S960 grade steel is investigated experimentally and numerically using conventional stress-based methods and a novel multi-parametric fatigue design approach known as the 4R method (see bolded *R* and *r* letters as an introduction to the name) [3,4]. In prior studies, the 4R method has shown high accuracy in predicting the fatigue strength of welded joints in the as-welded (ASW) and high-frequency mechanical impact (HFMI)-treated conditions [4,5], yet only with very limited scope for the TIG-dressed condition [6]. The present study aims to further verify and study the applicability of the 4R method for predicting the fatigue strength of TIG-dressed ultra-high-strength steel (UHSS) fillet weld joints under constant amplitude (CA) tensile loading with different applied stress ratios. The applied experimental fatigue test data were comprehensively described by Skriko *et al.* [7]. The results of the 4R procedure for the fatigue test data by Skriko *et al.* are here compared to data from the literature, namely Hensel *et al.* [8,9], who studied TIG-dressed longitudinal stiffeners made of S355 and S960 steels.

The fatigue strength of a welded joint can be improved by post-weld treatments, e.g. TIG-dressing. Post-weld treatment methods can be divided into two groups: Methods for the improvement of the weld profile, i.e. the weld toe, and methods for the improvement of the state of residual stresses [2,10]. The TIG-dressing technique modifies both the profile of the weld toe as well as the residual stress level at the weld toe. On the weld toe, remelting can also remove initial cracks, undercuts, and other imperfections that can cause premature fatigue failures. TIG-dressing reduces the local stress concentration at the weld toe due to the smoother transition between the weld and base materials provided by remelting. In addition, remelting also has an influence on the microstructure of the material. Skriko *et al.* observed that TIG-dressing causes a significant decrease in hardness in the fusion lines and heat affected zones (HAZs) of S960 MC weldments, which might have an effect on fatigue crack initiation and thus the fatigue strength of the structure [7].

In the literature, many studies have shown the improvement of fatigue strength obtained by using TIG-dressing [10–17]. Huo *et al.* [13] reported that the fatigue strength increased by 37 % and the fatigue life by 2.5 times after TIG-dressing. Haagensen *et al.* [10] proposed an increase in the allowable stress range by a factor of 1.3, corresponding to a factor of 2.2 on fatigue life (*S-N* curve slope of $m = 3$). Pedersen *et al.* [15] found that fatigue strength increased by 38 % for T-joints made of S700 high-strength steel. The International Institute of Welding (IIW) [2] includes recommendations for fatigue strength improvement using TIG-dressing only for the nominal and structural hot spot stress methods (Table 1). An improved FAT class for the nominal stress method is determined using an improvement factor of 1.3. In this study, the fatigue class is FAT80 for non-load-carrying cruciform joints in ASW condition according to the IIW recommendations [2]. This signifies an improved fatigue class FAT100 (a two FAT class improvement) for TIG-dressed joints. The improvement is limited to a maximum possible fatigue class value of FAT112. In addition, the recommendation is applicable for welded steels with a yield strength of up to 900 MPa. Guidelines and standards give FAT values that represent the stress range at load cycles $N = 2 \cdot 10^6$ for a survival probability of 97.7 %. FAT classes for the welded joints also assume a high residual stress state ($R \approx 0.5$). In the IIW recommendations [2], the slope of the *S-N* curve is determined to be $m = 3$. Experimental fatigue tests for TIG-dressed joints have shown that the slope is typically larger (higher *m* value) than $m = 3$. Yildirim *et al.* [11] presented improved fatigue classes for TIG-dressed joints made of steel grade $235 < f_y < 950$ MPa using the nominal stress method, whereby they investigated longitudinal attachment, transverse non-load-carrying joints, and butt joints. The proposed fatigue class for TIG-dressed transverse non-load-carrying joints for steel grade $750 < f_y < 950$ MPa was FAT140 (Table 1) with an *S-N* curve slope of $m = 4$. In this study, the steel grade is slightly over 950 MPa; nevertheless, the FAT class proposed by Yildirim *et al.* [11] is studied. For the structural hot spot stress method, the improvement fatigue class is FAT125 for TIG-dressed joints according to the IIW recommendations [2]. Unfortunately, improved FAT classes are not available for the ENS method. A fictitious radius of rounding of $r = 1$ mm is suitable for ASW joints with a sharp weld toe. However, for TIG-dressed welds with a smooth transition between the weld and base materials, a radius of 1 mm is unsuitable. Baumgartner *et al.* [18] studied TIG-dressed joints using local stress approaches. They studied the fatigue test data using the theory of critical distance (TCD) and the scatter of values on a path perpendicular to the weld surface. Two different ways to define the fatigue strength of TIG-dressed joints were proposed: 1) The position of the weld toe: The stresses determined at a distance of $a = 0.7$ mm below the surface and fatigue class FAT160 can be used, and 2) the position of the maximum stress: The stresses determined at a distance of $a = 0.6$ mm below the surface and fatigue class FAT180 can be used [18]. The critical distance *a* was determined by minimizing the scatter of the *S-N* curve and the lowest scatter was chosen.

Table 1. FAT classes for non-load-carrying cruciform joints improved by TIG-dressing [2,11,18]

Method	FAT (ASW)	FAT (TIG-dressed)	m	Reference
Nominal stress method				
for all steel grades	80	100	3	IIW [2]
$750 < f_y < 950$ MPa	-	140	4	Yildirim [11]
Hot spot method				
	100	125	3	IIW [2]
ENS method				
	225	-	3	IIW [2]
TCD				
1) Position of the weld toe (a = 0.7 mm)	-	160	4	Baumgartner [18]
2) Position of the max. stress (a = 0.6 mm)	-	180	4	Baumgartner [18]

THEORETICAL BACKGROUND OF THE 4R METHOD

4R analysis procedure

The 4R method is a novel multi-parametric fatigue design approach that differs from conventional stress-based approaches, i.e. the nominal stress, structural hot spot stress and effective notch stress methods, because it takes into account the effect of the material ultimate strength (R_m), joint geometry (K_t and r_{true}), applied stress ratio (R) and residual stresses (σ_{res}). The basic principles and procedures of the 4R concept were described by Nykänen *et al.* [3,4] and Björk *et al.* [19]. The 4R method was also studied for steel grade S1100 in ASW and post-weld treated conditions by Ahola *et al.* [6,20], for variable amplitude loading by Nykänen *et al.* [21], and for duplex and super-duplex stainless steels by Björk *et al.* [5].

The 4R method is a combination of the ENS, Smith-Watson-Topper (SWT), and local strain methods. The 4R method is based on the local stress ratio (R_{local}), which is the local stress ratio at the notch root and comprises the effect of ultimate strength (R_m), joint geometry (fatigue notch factor K_f and measured weld toe notch radius r_{true}), applied stress ratio (R), and residual stress state (σ_{res}). The Ramberg-Osgood (R-O) elastic-plastic material model and Neuber's rule are used to approximate the material cyclic behavior at the notch of the weld toe and to calculate local stress ratio. The material cyclic behavior is simulated considering the applied stress ratio, material ultimate strength, residual stress, and quality and shape of the weld toe. In this study, the R-O material parameters E = 200 GPa, n = 0.15 and $H = 1.65 \cdot R_m$ [22] are used with ideal kinematic hardening.

Local maximum stress (σ_{max}) of the cyclic behavior can be calculated using Equations 1 and 2, in which respectively the R-O equation for monotonic loading and the Neuber hyperbolae are used. The input parameter, effective notch stress range $\Delta\sigma_k$, can be defined using e.g. finite element (FE) analysis with the fictitious notch radius (ENS method).

$$\varepsilon = \varepsilon_e + \varepsilon_p = \frac{\sigma}{E} + \left(\frac{\sigma}{H}\right)^{\frac{1}{n}} \tag{1}$$

$$\varepsilon = \frac{\left(\frac{\Delta\sigma_k}{1-R} + \sigma_{res}\right)^2}{\sigma E} \tag{2}$$

The residual stress level (compression or tension stress) also has an effect on the local maximum stress and, consequently, the hysteresis stress loop can change significantly. Due to lack of knowledge, the conventional methods assume a tensile residual stress equal to the material yield strength for joints in

the ASW condition. This is a reasonable assumption for joints made of mild steels, but in UHSS weldments in a post-weld treated state, for example, this assumption can be incorrect, i.e. too conservative. For small test specimens made of UHSS, the welding residual stresses after welding can be significantly lower than the yield strength [23] and the scope of post-weld treatments is to generate a compressive residual stress level. In TIG-dressed UHSS weld joints, the compressive residual stresses are typically lower than in corresponding HFMI-treated joints [20]. The 4R method numerically accounts for the residual stresses. However, the method is not sensitive to the exact values of residual stresses; instead, the question is whether they are relatively high or low [21].

The local stress range ($\Delta\sigma$) at the notch of the weld toe is defined using Equations 3 and 4, whereby the cyclic behavior of the R-O material model and Neuber counterhyperbolae are used to approximate the material elastic-plastic behavior. Thereafter, the local minimum stress can be calculated using $\sigma_{min} = \sigma_{max} - \Delta\sigma$.

$$\Delta\varepsilon = \Delta\varepsilon_e + \Delta\varepsilon_p = \frac{\Delta\sigma}{E} + 2\left(\frac{\Delta\sigma}{2H}\right)^{\frac{1}{n}} \tag{3}$$

$$\Delta\varepsilon = \frac{\Delta\sigma_k^2}{\Delta\sigma E} \tag{4}$$

Based on the cyclic elastic-plastic behavior, the local stress ratio R_{local} can be obtained ($R_{local} = \sigma_{min} / \sigma_{max}$). The local stress ratio can be calculated when the local minimum and maximum stresses are defined corresponding to the effective linear-elastic notch stress range, $\Delta\sigma_k$. A more detailed description of the computation of local stress ratio, and the procedure of the 4R method are presented by Nykänen *et al.* [4].

Figure 1 presents the characteristics and the subsequent notch stress ranges of fillet-welded joints in the ASW and TIG-dressed conditions as well as the effect of the residual stress level and the possible relaxation of it on the local cyclic behavior and stress ratio at the notch of the weld toe in general.

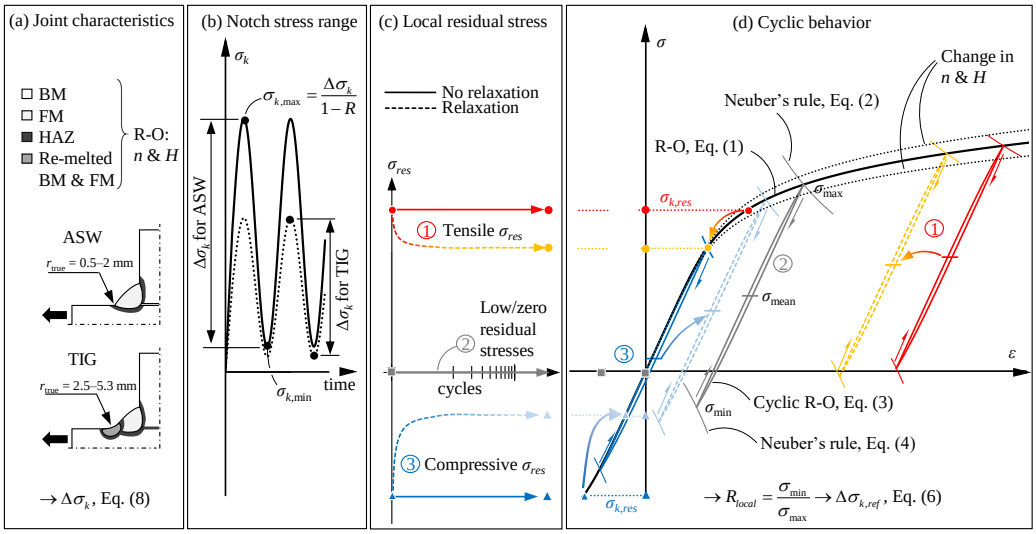

Figure 1. Cyclic behavior and local stress ratio definition: (a) The characteristics and (b) subsequent notch stress ranges of a fillet-welded joint in the ASW and TIG-dressed conditions, and (c) the effect of the residual stress level and the possible relaxation of it on (d) the local cyclic behavior and stress ratio at the notch of the weld toe.

The effective notch stress range $\Delta\sigma_k$ can be defined using FE analysis, analytical stress concentration factor (SCF) formulas, or artificial neural network (ANN) based analysis [24]. In this study, the effective notch stress ranges are calculated using FE model based on the fictitious notch radius r = 1 mm and $r = r_{true}$ + 1 mm. Ahola *et al*. [6] initially presented that the fictitious notch radius $r = r_{true}$ + 1 mm shows good accuracy for the fatigue strength prediction for TIG-dressed joints made of S1100 steel. Detailed descriptions of the used ENS model and the definition of the effective notch stress range are presented in "Numerical Analysis" chapter.

The 4R method differs from conventional methods that have a linear *S-N* curve (log-log scale). The 4R method gives a "continuous" design curve for the fatigue assessment of welded structures based on the local stress ratio, R_{local} [3]. The "continuous" *S-N* curve is different for all combinations of the 4R parameters (R_m, R, r, σ_{res}). Therefore, the 4R method does not need any correction or reduction factors. Fatigue life in the 4R method can be presented as follows:

$$N_f = \frac{C_{ref}}{\left(\Delta\sigma_{k,ref}\right)^m} = \frac{C_{ref}}{\left(\frac{\Delta\sigma_k}{\sqrt{1-R_{local}}}\right)^m} \tag{5}$$

where m is the slope of the reference *S-N* curve and C_{ref} is the fatigue capacities. In equation, the reference stress range $\Delta\sigma_{k,ref}$ is converted using the Equation 6.

The reference S-N curve

The continuous *S-N* curve can be converted to a linear *S-N* curve (log-log scale) by modifying the experimental fatigue test data ($\Delta\sigma_{k,i}$ and $N_{f,i}$) to a reference coordinate system using Equation 6. The effect of the local stress ratio R_{local} on the fatigue strength can be calculated using the SWT damage parameter [22]. This SWT parameter is widely used to account for the mean stress effect [25]. When the reference value of the local stress ratio is selected as $R_{local,ref}$ = 0, the converted equation is in the form:

$$\Delta\sigma_{k,ref} = \Delta\sigma_k \frac{\sqrt{1-R_{local,ref}}}{\sqrt{1-R_{local}}} = \frac{\Delta\sigma_k}{\sqrt{1-R_{local}}} \tag{6}$$

A more detailed description of the 4R method is presented by Nykänen *et al.* [4]. If experimental fatigue tests have a different R_{local} value due to a different stress concentration, residual stress state or magnitude of loading, the reference stress range $\Delta\sigma_{k,ref}$ must be calculated separately for each data point. Thereafter, the curve-fitting can be done using a standard [2] or MSSPD-fitting procedure (minimization of the sum of squared perpendicular distances from a line), which is a special case of Deming regression [26]. The MSSPD-fitting procedure is a mathematically more accurate approach compared to the standard method because it observes errors in both axis directions. Previous studies have shown that this curve-fit procedure is suitable for laboratory tests in which the applied stresses are not fully deterministic (i.e. include some randomness) [3]. The applied stress can vary locally and this causes a variation in the stress range. The prior study [3] also showed that a higher coefficient of determination value was received when using the MSSPD approach, instead of the standard approach. In addition, the reference stress used in the 4R analysis contains more uncertainty than the stress used in the conventional methods, as the reference stress is calculated using the local stress ratio R_{local} influenced by the 4R parameters. The slope of the MSSPD-fitting procedure is typically shallower (higher m value) than the slope obtained using the standard procedure [3].

The 4R analysis of this study is based on the master *S-N* curve defined by Nykänen *et al.* [4]. This master *S-N* curve was originally determined for butt-welded joints in the ASW condition under CA tensile loading. The master *S-N* curve was defined using approximately 800 experimental fatigue test results for butt-welded joints. In previous studies, this same master *S-N* curve was also used for different joint types (non-load-carrying cruciform joints and T-joints and longitudinal non-load-carrying joints) [4–6,21]. In addition, HFMI-treated weld joints made of UHSS and duplex steels were investigated using this master *S-N* curve [4,5].

When using the MSSPD-fitting procedure, the master *S-N* curve parameters are:

$$\Delta\sigma_{k,\mathrm{ref}}^{m} N_f = C_{\mathrm{ref}}, \text{ where } \; m = 5.85, \; C_{\mathrm{ref,mean}} = 10^{21.59} \; \text{ and } \; C_{\mathrm{ref,char}} = 10^{20.83} \;, \qquad (7)$$

where m is the slope of the reference *S-N* curve and $C_{\mathrm{ref,mean}}$ and $C_{\mathrm{ref,char}}$ are the mean and characteristic (95 % survival probability) fatigue capacities, respectively.

EXPERIMENTAL FATIGUE TESTS

In this section, the used materials, studied test specimens, applied measurements, and test setup are briefly introduced along with the compared fatigue test results collected from the literature. The total number of fatigue test specimens was 34, of which 23 failed in the investigated area, i.e. the TIG-dressed weld toe. In this study, only these 23 test specimens are re-reported and analyzed. More information related to the execution of the experimental fatigue tests can be found in the article by Skriko *et al.* [7].

Materials

Experimental fatigue tests were carried out for non-load-carrying cruciform joints made of direct-quenched UHSS S960 MC steel with a plate thickness of t = 8 mm. Böhler Welding Union X96 solid wire was used as a filler metal, which is nominally a slightly undermatching filler material for S960 steels [7]. The mechanical properties of the base material and filler metal are presented in Table 2.

Table 2. Mechanical properties of the base material and filler metal (minimum values) [7]

Material	Type	Yield strength $R_{p0.2}$ [MPa]	Ultimate strength R_m [MPa]	Elongation A_5 [%]	Impact strength T [°C]	KV [J]
S960 MC	nominal	960	980–1250	7	-40	27
	measured	1032	1125	10	-40	56
Union X96	nominal	930	980	14	-50	47

Test specimens

The test specimens consisted of 8 mm thick base plates with equal-thickness transversal attachments. The main dimensions and shape of the non-load carrying cruciform joints are presented in Figure 2. The starting and ending point areas of the welding and TIG-dressing were removed by sawing and machining prior to the fatigue tests (dashed lines in Figure 2). A robotized gas metal arc welding (GMAW) process was used to weld the fatigue test specimens, and the TIG-dressing was done manually for all specimens according to the recommendation by Haagensen *et al.* [10]. For every run, the heat input of the GMAW and TIG-dressing was 1.0 kJ/mm and 0.5 kJ/mm, respectively. Table 3 presents the welding parameters used in this study. The welding and TIG-dressing parameters were kept constant in order to ensure similar geometric and metallurgical properties for all fatigue test specimens. The TIG-dressing was carried out only for the weld toes of the base plate side because those were the critical weld toes in the studied non-load carrying cruciform joint (Figure 3). The nominal throat thickness was

a = 5 mm in all fillet welds. Typical geometries of the joint in ASW and TIG-dressed condition are presented in Figure 3. Detailed descriptions of the welding procedure and TIG-dressing parameters can be found in the article by Skriko *et al.* [7].

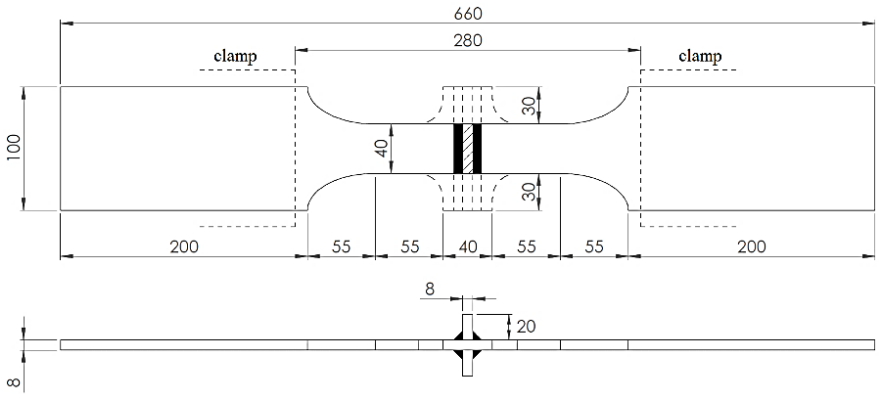

Figure 2. Dimensions of the test specimens (all dimensions in mm) [7].

Table 3. Welding and TIG-dressing parameters

Process	Current [A]	Voltage [V]	Travel speed [mm/s]	Wire feed [m/min]	Heat input [kJ/mm]
GMAW	241–258	31.3–31.7	5.9	13.2	~ 1.0
TIG-dressing	180	13.2	2.4–3.4	-	~ 0.5

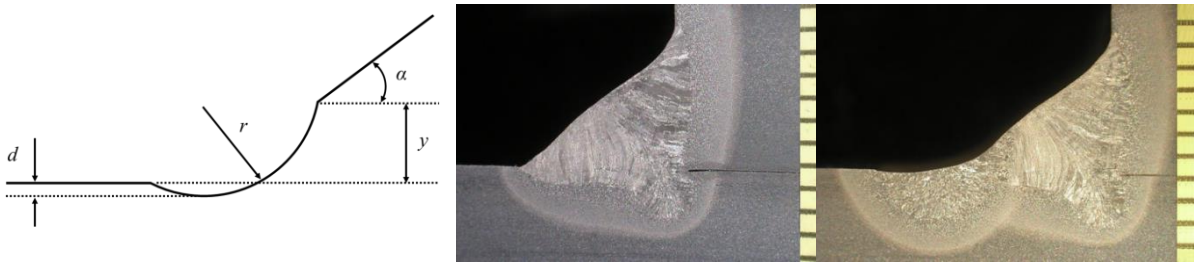

(a) (b) (c)

Figure 3. (a) Geometric factors and variables of TIG-dressed specimens; (b) geometry of the weld toe before and (c) after TIG-dressing [7].

Measurements

Before fatigue testing, the geometry of the weld profiles, residual stresses, and material hardness of the specimens were measured. Residual stresses were measured from the surface of the selected specimens using an X-ray diffractometer. Residual stresses, parallel to the loading direction, were measured before and after TIG-dressing along the centerline of each specimen (Figure 4). The measurements were conducted starting from the weld toe in the direction of the base plate. Figure 4 shows the changes to the distribution and magnitude of the residual stresses before and after TIG-dressing. The residual stresses at the weld toe tend to be slightly in tension in the ASW condition for UHSS. Based on this study, after TIG-dressing, the residual stresses are mainly in compression at the weld toe. Table 5 presents the analyzed residual stress levels. These values were selected according to the ruptured weld toe. The variations of the residual stress measurements were significant, from +250 to -481 MPa. However, only one of these residual stress measurements gave a result in tension. Nevertheless, TIG-dressing improved the residual stress level for each test specimen and each weld toe.

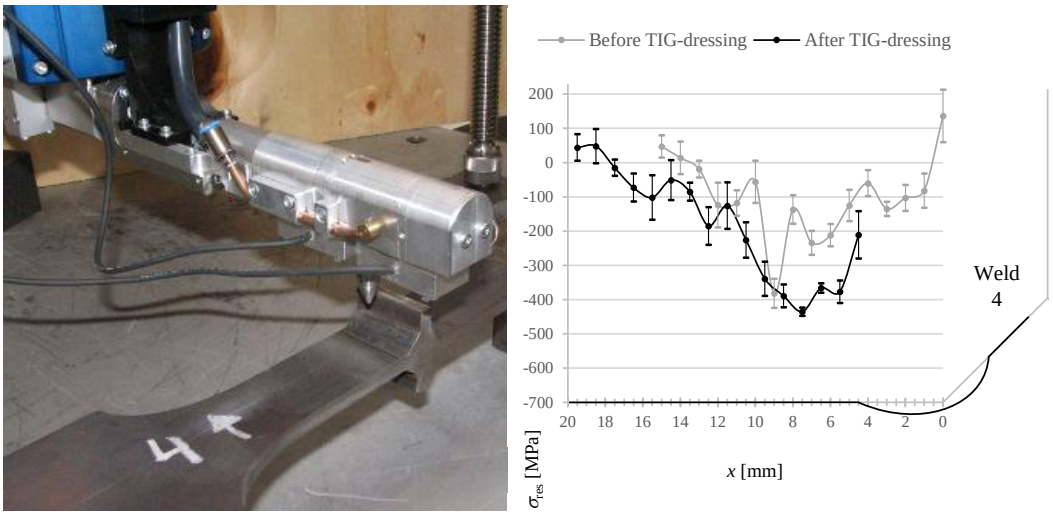

Figure 4. Residual stress (a) measurement setup and (b) distribution along the surface [7].

The geometrical changes after TIG-dressing can be defined by measuring the weld toe radius, weld toe angle, and undercut of the weld (Figure 3a). These parameters of the weld profiles were measured in the article by Skriko *et al.* [7] using a two-dimensional laser measuring system. Table 5 presents the results of the geometry measurements. TIG-dressing seemed to leave the weld toe with the smoother transition between the weld and the base materials. Nevertheless, the transition geometry of the TIG-dressed weld toe varied significantly between the test specimens. The typical radius of the TIG-dressed weld toe was 2.5–5.3 mm, whereas the rounding under ASW conditions was 0.5–2 mm [7]. Based on the measurements of the 23 analyzed test specimens, the average value of the weld notch radius after TIG-dressing was 3.7 mm. Similar results were found in previous research by Ramalho *et al*. [16], Rudolph *et al*. [17] and Tateishi *et al*. [27], as presented in Table 4.

Table 4. Literature review of the weld toe radii (mm) in ASW and TIG-dressed conditions

	ASW	TIG
Skriko *et al*. [7]	0.5–2.0	2.5–5.3
Ramalho *et al*. [16]	4.1 (mean)	6.3 (mean)
Rudolph *et al*. [17]	0.1–1.4	2.9–10.0
Tateishi *et al*. [27]	0.9 and 1.8 (average)	3.8 and 4.4 (average)

The hardness of the weld areas was measured with the Vickers method (HV) in the TIG-dressed condition. The results are presented in Figure 5, where they clearly show the macrogeometry of the fillet weld and TIG-dressed region. Due to softening, the HAZs of the fillet weld and the TIG-dressing have approximately 10–20 % lower hardness values than the base material. In addition, minor softening can be observed in the fusion lines. The hardness in the TIG-dressing areas has increased by approximately 20 % (350 HV). Detailed descriptions of the measurements can be found in the article by Skriko *et al.* [7].

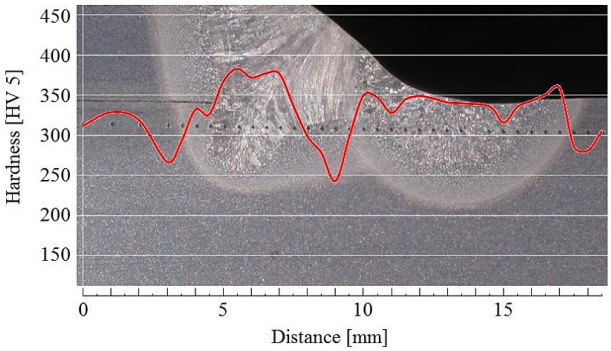

Figure 5. Hardness distribution of the TIG-dressed fillet weld joint [7].

Test set-up

All specimens were carried out under CA tensile loading. The fatigue tests were performed using a load-controlled servo-hydraulic test rig. Each specimen was equipped with a strain gage to measure the magnitude of macrogeometric bending stresses induced by the angular distortion of the specimens. The maximum stress levels in the tests were between $0.5 \times f_y$ and $0.8 \times f_y$ (f_y = 960 MPa) and the stress ratios were R = 0.1–0.6. The maximum stress levels were obtained using the strain gage measurements. The failure criterion for the test specimens was a total fracture. Detailed descriptions of the test setup can be found in the article by Skriko *et al.* [7].

Fatigue test results

The fatigue test data of the experiments are summarized in Table 5, which presents the applied stress ratio, ultimate strength of the material, measured radius and undercut of the weld toe, residual stress, nominal stress range, fatigue life, and failure location. The residual stresses after TIG-dressing are presented only for the measured specimens. The presented and analyzed residual stress values were selected according to the place (the weld toe) of crack initiation.

Table 5. Fatigue test data and measurements

ID	Weld toe radius r [mm]	Undercut d [mm]	Stress ratio R [-]	Residual stress* σ_{res} [MPa]	Nominal stress $\Delta\sigma_{nom}$ [MPa]	Fatigue life $N_{f,\,test}$ [$\cdot 10^3$]	Failure location RT = region of the TIG-dressing FLT = fusion line of the TIG-dressing BM = base material
X1	0.7	0.08	0.37	-38	412	191	FLT (side of the weld)
X2	2.4	0.08	0.25		527	107	RT
X3	2.5	0.00	0.51		381	220	RT
X4	2.8	0.00	0.50	-320	323	241	RT
X5	3.1	0.00	0.38		444	159	RT
X6	3.5	0.15	0.50		377	168	RT
X7	3.6	0.04	0.38		347	381	RT
X8	3.7	0.10	0.26	250	486	151	RT
X9	3.7	0.15	0.12		559	134	RT
X10	3.7	0.11	0.40	-390	430	256	FLT (side of the weld)
X11	3.7	0.14	0.25	-176	490	184	FLT (side of the weld)
X12	3.7	0.00	0.10		632	54	RT
X13	3.8	0.00	0.24		354	615	RT
X14	3.9	0.00	0.25		551	82	RT + FLT (side of the BM)
X15	4.1	0.10	0.10	-178	434	227	RT
X16	4.1	0.00	0.38		441	267	RT
X17	4.2	0.11	0.25		414	266	RT
X18	4.3	0.00	0.12		568	116	RT
X19	4.3	0.29	0.50	-271	327	611	FLT (side of the weld)
X20	4.5	0.00	0.10		663	51	RT
X21	4.7	0.18	0.61		299	703	RT
X22	4.9	0.18	0.07	-84	460	132	FLT (side of the weld)
X23	5.3	0.15	0.09	-481	510	197	RT

* Surface residual stress measured before test

Experimental fatigue test data from the literature

The fatigue test results of of Skriko *et al.* [7] are compared to the literature data presented by Hensel *et al.* [8,9], who studied TIG-dressed longitudinal stiffeners made of S355 and S960 steels. Next, the analyzed test data are briefly introduced. Detailed results and descriptions can be found in the original references. The fatigue data obtained by Hensel *et al.* included 42 test results with stress ratios of R = -1. These specimens consisted of 12 mm thick plates with longitudinal attachments. The attachment length was 150 mm and the main plate width was 60 mm. Because the weld size was not reported, fillet welds with a throat thickness of 5 mm and a flank angle of 45° were approximated based on the macrograph. The specimens were subjected to axial loading and a reported angular misalignment of 0.4° was observed. The specimens were in the TIG-dressed condition, whereby the measured weld toe radius was 5–10 mm. In this study, the worst-case assumption for the weld toe radius was used (r_{true} = 5 mm). The reported material strength values were R_m = 568 MPa and $R_{p0.2}$ = 390 MPa and R_m = 1070 MPa and $R_{p0.2}$ = 1000 for S355 and S960 grade steels, respectively. Unfortunately, the welding residual stresses were not reported for every test specimen. Only one measured residual stress value was reported for each of the steels, and these are used for the 4R analysis (σ_{res} = 20 MPa for S355 and σ_{res} = 140 MPa for S960). Although many experimental studies focusing on the fatigue strength improvement of welded joints using TIG-dressing exist, the details needed for the 4R analysis, such as weld toe radii, angular misalignments, residual stresses, and weld profiles, are not reported precisely enough in these publications; therefore, such data and results from the literature were excluded from this study.

NUMERICAL ANALYSIS – EFFECTIVE NOTCH STRESS MODEL

The ENS method is based on modelling a fictitious rounding of the weld toe with an appropriate radius [28–31]. The fictitious radius of rounding can be defined as $r = r_{true} + 1$ mm. For low-strength steels, Radaj *et al.* [22] presented a linear elastic stress analysis of a welded joint modelled with a worst-case notch radius of r = 1 mm ($r = r_{true} + \rho^* \cdot s$ = 1 mm). This presented radius corresponds to a sharp weld toe when r_{true} = 0. This assumption is based on a theoretical determination that takes into account the micro-structural support length ρ^* = 0.4 and the factor s = 2.5. The fatigue class of the ENS method for ASW joints with a plate thickness $t \geq 5$ mm is FAT225 ($N = 2 \times 10^6$ and slope m = 3) when the maximum principal stress criterion is used.

A statistical analysis of the geometric variables and a considerable amount of FE models were carried out in a previous study by Skriko *et al.* [7]. TIG-dressed cruciform joints were analyzed using the commercial ABAQUS and ANSYS software using a two-dimensional plane strain FE model with the quadratic element order and quadrilateral element shape. The geometry, boundary condition, and load of the symmetrical ENS model are presented in Figure 6. The linear elastic material model E = 200 GPa and ν = 0.3 were used with the small displacement theory. In this study, the effective notch stresses at the weld toe are determined using the fictitious notch radius r = 1 mm and $r = r_{true}$ + 1 mm at the weld toe. Radaj *et al.* [22] showed that the notch radius for high-quality welds corresponds to an enlarged radius of rounding $r = r_{true}$ + 1 mm. In this study, the TIG-dressing is assumed to induce only geometrically effect for the weld toe (no material effects). Skriko *et al.* [7] found that the weld toe radius, r values has the most significant effect on the SCF. Due to this observation, the flank angle was set to 45°, which is also recommended by Hobbacher [2], and the value y was set to 1.5 mm (Figure 3). The recommended element size is 0.25 mm or smaller in the case of a 1 mm radius and parabolic element [2,32,33]. In this study, the size of the elements at the weld toe was smaller than 0.15 mm. Figure 6 shows a representative ENS model and element mesh used in this study. Such an ENS model gives the SCF for membrane stress as K_{tm} = 1.47 and for bending as K_{tb} = 1.24 when the averaged fictitious notch radius $r = r_{true,\ average}$ + 1 mm = 4.7 mm at the weld toe and the weld undercut d = 0 mm are used. The maximum principal stress criterion was used for the ENS analyses. The effect of the undercut, $d = 0 \rightarrow 0.15$–0.25, is approximately 5–8 % for K_{tm} values and 11–14 % for the K_{tb} values when the fictitious notch radius is 4–5 mm. Naturally, when the undercut increases, the SCF also

increases. For the fictitious notch radius r = 1 mm, the SCF for membrane stress was K_{tm} = 2.37 and for bending stress it was K_{tb} = 1.80.

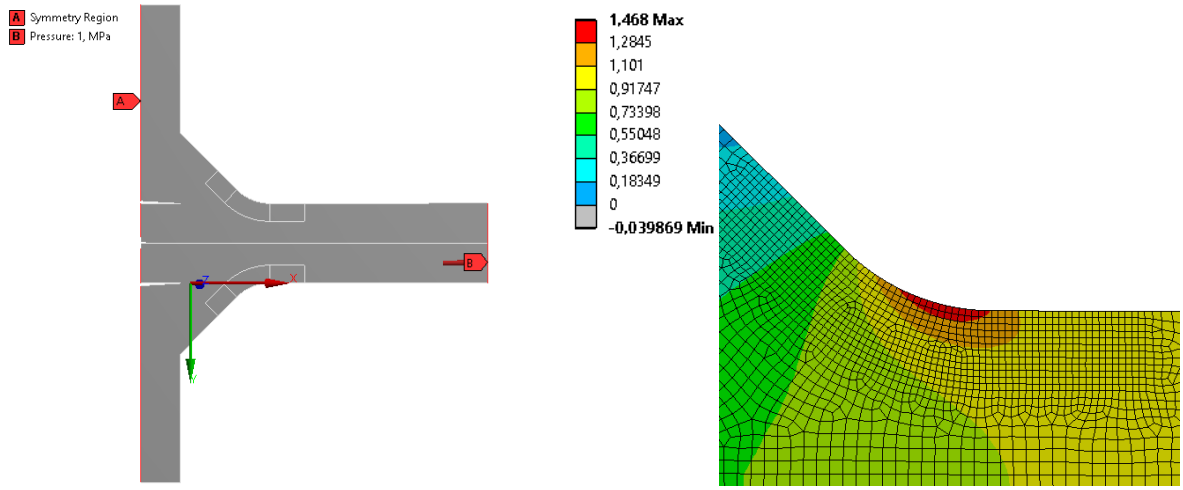

(a) (b)

Figure 6. (a) FE model of the TIG-dressed fillet weld using the averaged fictitious notch radius r = $r_{true,\ average}$ + 1 mm = 4.7 mm at the weld toe and a weld undercut of d = 0 mm. (b) Used mesh size and calculated K_{tm} value for membrane stress using the maximum principal stress criterion.

The measured weld geometries, i.e. the radius and undercut of the weld toe, were modelled but no angular misalignment. Instead, the bending stress caused by the angular distortion was defined by the strain gage measurement. The effect of the bending stress on the effective notch stress is separately calculated using Equation (8). Each different model was analyzed separately with both axial and bending loading, and the SCFs for both loadings were defined. The K_{tm} and K_{tb} values were obtained using the maximum principal stress criterion. The membrane stress, $\Delta\sigma_m$, for each test specimen is the applied stress range and the bending stress, $\Delta\sigma_b$, is calculated as $\Delta\sigma_b = \Delta\sigma_{HS} - \Delta\sigma_m$. In that case, the effective notch stress range can be calculated as follows ($K_f \approx K_t\,(r \geq 1\text{mm})$):

$$\Delta\sigma_k = K_{t,m}\Delta\sigma_m + K_{t,b}\Delta\sigma_b \tag{8}$$

The longitudinal attachment by Hensel *et al*. [8,9] was modelled using the fictitious notch radius r = 1 mm and r = r_{true} + 1 mm at the weld toe when the measured weld toe radius was 5 mm. For the fictitious notch radius r = 1 mm, the SCF for the membrane stress was K_{tm} = 3.34 and for bending stress it was K_{tb} = 2.99. The structural SCF of the test specimens with an angular misalignment angle of 0.4° was K_s = 1.40. For the fictitious notch radius of r = r_{true} + 1 mm = 6 mm, the SCF for membrane stress was K_{tm} = 1.92 and for bending stress it was K_{tb} = 1.77.

RESULTS

The analyzed experimental fatigue test data are presented in Table 6. The test results were analyzed using the nominal stress, structural stress (hot spot), effective notch stress, and 4R methods. The nominal stress ranges were defined according to the monitored force values of the servo-hydraulic test rig and the measured cross-section dimensions of the specimens. The structural stress ranges were obtained on the basis of the strain gage measurements. Based on the strain gage measurements and the shape measurements of the test specimens, no significant angular misalignments were found. The

structural stress concentration factor of the test specimens was K_s = 1.01–1.05. The results of the ENS and 4R methods were obtained using the FE analyses and SCF values K_{tm} and K_{tb} (Equation 8). In Table 6, the effective notch stress ranges and SCFs of the ENS method were defined using the measured notch radii at the weld toe and an undercut value of d = 0 mm. In this case, the fictitious notch radius in a single FE model was $r = r_{true} + 1$ mm and it was different for each of the test specimens.

The results of the 4R method in Table 6 were transferred into the reference notch stress system using the averaged fictitious notch radius $r = r_{true,\ average} + 1$ mm = 4.7 mm and the undercut value d = 0 mm at the weld toe for each of the test specimens. In that case, the calculated K_t values for the membrane and bending stresses were K_{tm} = 1.47 and K_{tb} = 1.24 ($r = r_{true,\ average} + 1$ mm = 4.7 mm, d = 0 mm). In the 4R method, the local stress ratio R_{local} was calculated for each test specimen using Equations 1 to 4, and the notch stress range, $\Delta\sigma_k$, was converted to the reference system using Equation 6. The stress ranges, $\Delta\sigma_k$, the local stress ratio R_{local} and the stress ranges in the 4R reference system, $\Delta\sigma_{k,ref}$, are presented in Table 6.

In the 4R analysis, the worst-case assumption for residual stress, i.e. σ_{res} = -38 MPa, was used. The worst-case assumption is selected based on pre-study, where the 4R analysis were done using a different residual stress assumption. The worst-case assumption is conservative estimation for the residual stresses in the failure location. Because, the failure did not always occur at the center of the specimen where the measurements were done. Furthermore, the residual stresses could not be measured from the bottom of undercut, where the crack initiation and propagation typically occurred. The average value of the measured residual stresses was proved to be too non-conservative. Previous studies [6] have shown that worst-case assumption for the TIG-dressed joints is suitable. Same kind of assumption is used e.g. for the HFMI treated joints where a conservative assumption of $\sigma_{res} = 0.255R_m$ was given by Nykänen et al. [4] based on the measurements of existing studies. In the sub-section "Results - The 4R method" have presented also results of the 4R analysis using the measured residual stress levels with a different fictitious notch radius (r = 1 mm, $r = r_{true} + 1$ mm and $r = r_{true,\ average} + 1$ mm).

Table 6. Analyzed fatigue test data

ID	Nom	HS	ENS	4R			
	$\Delta\sigma_{nom}$ [MPa]	$\Delta\sigma_{hs}$ [MPa]	$\Delta\sigma_{ens}$* [MPa]	$\Delta\sigma_k$ ** [MPa]	R_{local} [-]	$\Delta\sigma_{k,ref}$ ** [MPa]	$N_{f,\ test}$ [$\cdot 10^3$]
X1	412	420	852	615	0.17	676	191
X2	527	576	924	836	-0.05	817	107
X3	381	379	618	557	0.30	667	220
X4	323	308	485	456	0.36	572	241
X5	444	478	713	695	0.13	744	159
X6	377	372	552	549	0.30	657	168
X7	347	358	524	524	0.24	600	381
X8	486	504	736	737	0.02	745	151
X9	559	605	877	879	-0.15	818	134
X10	430	440	644	644	0.17	708	256
X11	490	501	733	734	0.02	741	184
X12	632	692	1002	1004	-0.24	903	54
X13	354	365	530	534	0.12	570	615
X14	551	576	834	841	-0.05	821	82
X15	434	451	650	659	-0.05	643	227
X16	441	480	686	696	0.13	744	267
X17	414	432	613	631	0.08	658	266
X18	568	598	847	872	-0.15	813	116
X19	327	313	451	464	0.36	579	611
X20	663	629	896	933	-0.20	853	51
X21	299	306	424	448	0.44	599	703
X22	460	425	590	633	-0.06	614	132
X23	510	517	707	758	-0.11	720	197

* $r = r_{true} + 1$ mm

** $r = r_{true,\ average} + 1$ mm = 4.7 mm

Conventional methods

The test results were converted to *S-N* curves using the nominal stress, structural hot spot, and ENS methods. These results were compared to the *S-N* curves given by the current guidelines and design codes [1,2]. The applicable FAT classes for non-load-carrying cruciform joints improved by TIG-dressing are presented in Table 1. Figure 7 shows the test results and estimated *S-N* curves (red lines) using the standard curve-fitting procedure with fixed slope m = 4 for the nominal stress and structural stress methods. The test results were divided into five groups based on the measured weld toe radius. The fatigue test results were compared with the recommended FAT class (FAT100) for TIG-dressed joints given by Hobbacher [2]. Additionally, the results of the nominal stress method were also compared with the FAT140 *S-N* curve with a slope of m = 4 given by Yildirim *et al.* [11]. Both the characteristic and mean curves are presented for all *S-N* curves. The mean *S-N* curve (50 % survival probability) for the IIW recommendations [2] and Yildirim *et al.*'s [11] curves are estimated using a safety factor of 1.37 ($FAT_{mean} = FAT_{char} \cdot 1.37$). The fatigue test data in terms of the structural stresses were defined based on the strain gage measurements, whereby the bending stresses caused by angular misalignments of the test specimens were taken into account.

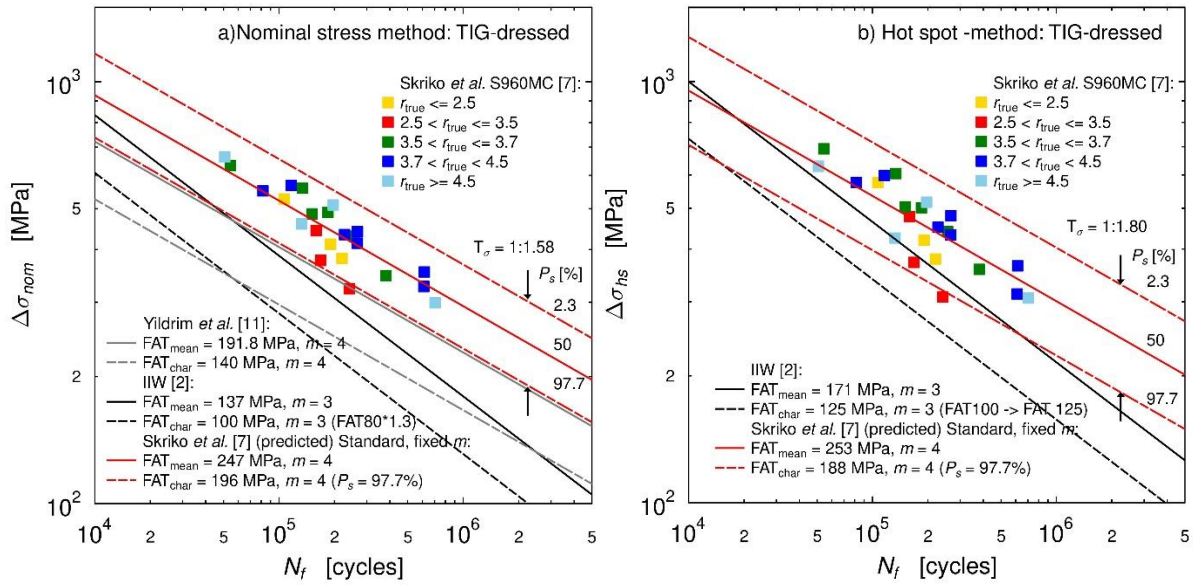

Figure 7. Fatigue test results and *S-N* curves for TIG-dressed weld joints using (a) the nominal stress and (b) the structural hot spot stress methods.

The test results for the ENS method are presented in Figure 8 for different geometry parameters. In order to investigate the fatigue strength analysis of TIG-dressed welded joints, the ENS stresses were defined in two different ways, namely $r = r_{true} + 1$ mm and r = 1 mm. In both cases, the undercut of the weld toe was d = 0 mm. The measured weld toe radii are presented in Table 5. The ENS stresses were obtained using FE analysis and the SCF (K_{tm} and K_{tb}) for each test specimen (Equation 8). In both ENS analyses, i.e. in Figure 8a with r = 1 mm and Figure 8b with $r = r_{true} + 1$ mm, the characteristic fatigue strength value FAT225 [2,34] and mean value FAT309 are presented. In addition, the estimated *S-N* curves (red lines) using the standard curve-fitting procedure with fixed slope m = 4 are shown.

In Figure 8b, all the test results lie on the mean FAT309 *S-N* curve given by the IIW recommendations [2], which means that the proposed radius of the notch $r = r_{true} + 1$ mm at the weld toe is appropriate for this study case. The test results are also all slightly above the characteristic FAT225 *S-N* curve and thus, are considered to be on the safe side.

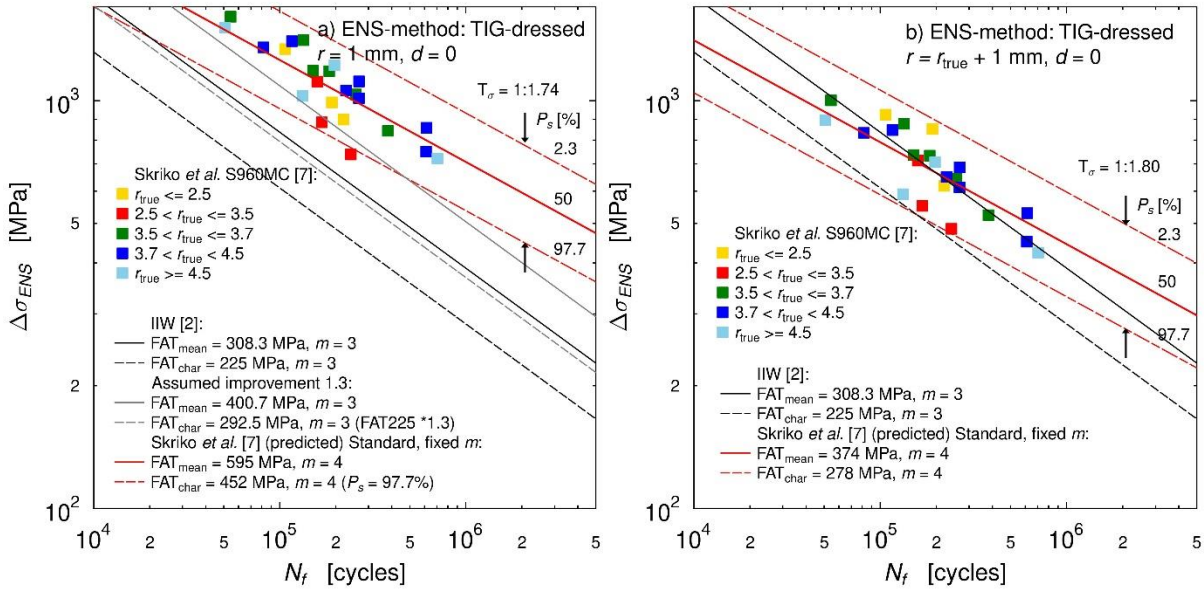

Figure 8. Fatigue test results and *S-N* curves for TIG-dressed weld joints in the ENS system using (a) the fictitious notch radius r = 1 mm and (b) $r = r_{true}$ + 1 mm at the weld toe.

A summary of the fatigue strengths derived using conventional methods is presented in Table 7. The *S-N* curve parameters FAT and *m* are defined based on the fatigue test data using the standard procedure with free and fixed slopes and the MSSPD curve-fitting procedure. The standard calculations were based on the statistical analyses presented by the IIW recommendations [2]. A scatter range T_σ are presented for all study cases.

Table 7. Values of *S-N* curves (FAT at $2 \cdot 10^6$ and *m*) using the standard regression analysis with a free slope and a fixed slope of m = 4, and the MSSPD-fitting procedure

Method	Standard, free m				Standard, fixed m				MSSPD			
	m	FAT_{char} [MPa]	FAT_{mean} [MPa]	1:T_σ* [-]	*m*	FAT_{char} [MPa]	FAT_{mean} [MPa]	1:T_σ* [-]	*m*	FAT_{char} [MPa]	FAT_{mean} [MPa]	1:T_σ* [-]
Nominal stress	2.8	149	192	1.65	4	196	247	1.58	3.5	180	226	1.56
Hots spot	2.4	124	174	1.97	4	188	253	1.80	3.3	168	224	1.77
ENS:												
r=1 mm	2.5	310	424	1.87	4	452	595	1.74	3.4	406	531	1.71
$r=r_{true}$+1 mm	2.4	182	255	1.96	4	278	374	1.80	3.3	246	327	1.77
$r=r_{true,aver.}$+1 mm	2.5	224	312	1.61	4	279	370	1.76	3.3	285	378	1.52

* The scatter range, P_s = 2.3%: P_s = 97.7%

The 4R method

In Figure 9 to Figure 11, the fatigue test data by Skriko *et al.* [7] are transferred into the reference notch stress system using the 4R method. The reference notch stress range, $\Delta\sigma_{k,ref}$, was calculated using Equation 6. The 4R fatigue assessment analyses were performed using the parameters presented in Table 5. The material certificated value of ultimate strength R_m =1125 MPa was used in all cases.

In Figure 9, the fatigue test data are presented using the fictitious notch radius r = 1 mm at the weld toe, the undercut value d = 0 mm, and the measured residual stress values σ_{res} = + 250 … - 481 MPa. The converted fatigue test data and estimation curves are also compared to the mean and characteristic master *S-N* curves (black lines) defined by Nykänen *et al*. [3,4]. Using the fictitious notch radius r = 1 mm, the results are clearly above the mean master curve in the reference coordinate system. On the other hand, the results follow the slope of the mean master *S-N* curve quite closely. The slope of the master *S-N* curve is m = 5.85 and the predicted slope of the converted fatigue test data is m = 5.08. Predicted *S-N* curves are presented for all test results and for two groups depending on the measured weld toe radius ($r_{true} \leq 3.7$ mm and $r_{true} > 3.7$ mm). Analyzed results for the specimens with the small weld radius ($r_{true} \leq 3.7$ mm) showed that the slope of the *S-N* curve is clearly deeper (m = 3.6) than specimen with large weld toe radius ($r_{true} > 3.7$ mm) which slope of the *S-N* curve is quite near to the slope of the master curve. This occurrence of the specimens with the small weld toe radius should be faced by further studies, which could enable an understanding of the dependency of the slope of the *S-N* curve on the weld toe radius.

The fatigue test results by Hensel *et al.* [8,9], re-analyzed with the 4R method with the fictitious notch radius r = 1 mm and the undercut d = 0 mm, are also presented in Figure 9. Hensel *et al*. [8,9] reported weld toe radii of r_{true} = 5–10 mm, and slightly higher fatigue strength is thus obtained for those results using the reference radius of r = 1 mm.

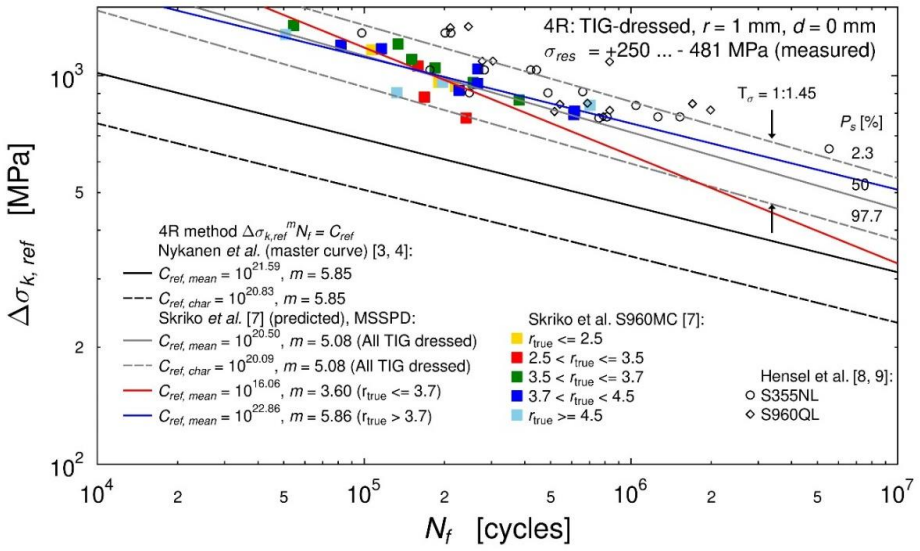

Figure 9. Fatigue test results and *S-N* curves for TIG-dressed weld joints in the 4R method using the fictitious notch radius r = 1 mm at the weld toe and the measured residual stress values.

Because the ENS analysis using the fictitious notch radius $r = r_{true}$ + 1 mm at the weld toe was appropriate, the fatigue data were also analyzed using the 4R method and the measured notch radii. In the results presented in Figure 10a and b, the SCF for the each of test specimens are modelled and analyzed using the fictitious notch radius $r = r_{true}$ + 1 mm based on measured values and the undercut d = 0 values. In Figure 10c, the SCF are modelled using the averaged fictitious notch radius $r = r_{true,average}$ + 1 mm. Figure shows how the scatter of the test specimens changes when the fictitious notch radius and the applied residual stress values changes. The converted fatigue data are closer to the mean master *S-N* curve [3] in all cases, but the scatter (T_σ = 1:1.52) is clearly smallest in Figure 10b. In all cases, the slope of the predicted *S-N* curve is quite close to the master *S-N* curve. The predicted slope of the reference *S-N* curve for all test specimens is m = 4.83 – 5.68. As all test results are quite near to the

mean master *S-N* curve, this means that the proposed radius of the notch $r = r_{true} + 1$ mm and $r = r_{true,\ average} + 1$ mm at the weld toe could be appropriate for this study case.

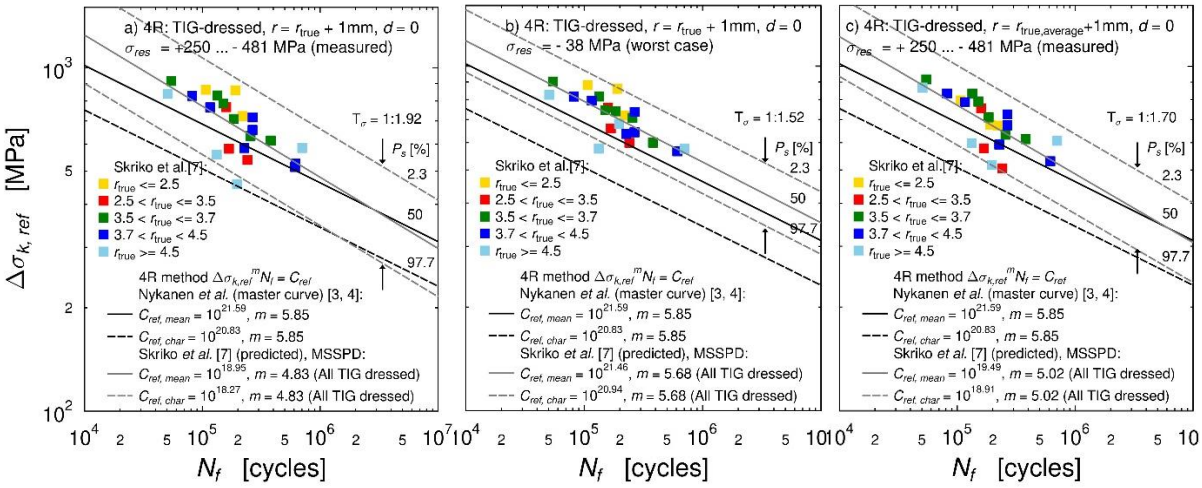

Figure 10. Fatigue test results and *S-N* curves for TIG-dressed weld joints in the 4R method using: a) the fictitious notch radius $r = r_{true} + 1$ mm and the measured residual stress values, b) the fictitious notch radius $r = r_{true} + 1$ mm and the worst-case assumption for residual stresses σ_{res} = -38 MPa, c) the averaged fictitious notch radius $r = r_{true,\ average} + 1$ mm and the measured residual stress values.

In Figure 11, the both fictitious notch radius and residual stresses are characterized. Due to the scatter in the residual stress measurements and the fixed location of the measurement with respect to the arbitrary location of crack initiation, the maximum value of the residual stress measurements was assumed to represent the residual stress in each test specimen. One tensile residual stress measurement +250 MPa was discarded as an outlier. The test results were converted to the reference coordinate system using the averaged fictitious notch radius $r = r_{true,\ average} + 1$ mm = 4.7 mm at the weld toe, the worst-case assumption for residual stress σ_{res} = -38 MPa, and the undercut value d = 0 mm. The undercut of the weld toe of d = 0 mm was chosen for all cases because the effect of the undercut of 0.15–0.25 mm on SCF is only 5–8 % when the notch radius is 4.7 mm. In half of the measurements, the undercut values were less than 0.1 mm.

The scatter range of T_σ = 1:1.40 of the converted fatigue data is clearly smaller using the characteristic values (Figure 11). The predicted *S-N* curve is quite near to the mean master *S-N* curve [3] and the slope of the predicted *S-N* curve is the same as the master *S-N* curve (m = 5.85). Thus, the assumption of characteristic values seems to be appropriate for TIG-dressed cruciform joints. The fatigue test results by Hensel *et al.* [8,9], analyzed using the 4R method with the fictitious notch radius $r = r_{true} + 1$ mm = 6 mm and the undercut d = 0 mm, are also presented in Figure 11. In this analysis, the results show a good correspondence with the predicted and master *S-N* curves.

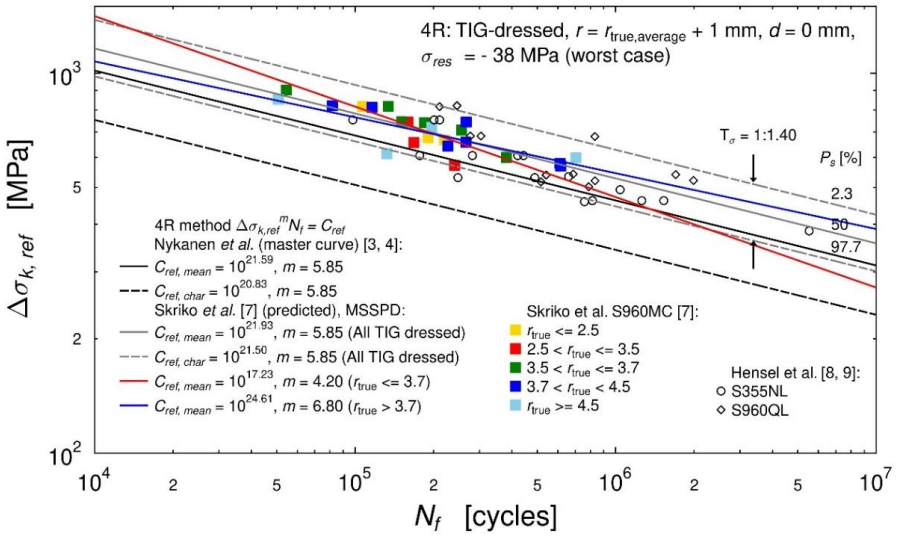

Figure 11. Fatigue test results and *S-N* curves for TIG-dressed weld joints in the 4R method using the averaged fictitious notch radius $r = r_{true,\ average} + 1$ mm at the weld toe and the worst-case assumption for residual stresses σ_{res} = -38 MPa.

Table 8 presents the calculated FAT values and the slopes of the reference *S-N* curves for the fatigue test data by Skriko *et al*. [7]. The *S-N* curve parameters *C*, FAT and *m* are defined from the fatigue test data using the standard procedure with free and fixed slopes and the MSSPD curve-fitting procedure. The standard calculations were based on the statistical analyses presented by the IIW recommendations [2]. A scatter range T_σ are presented for all study cases.

Table 8. FAT values and slopes of the 4R reference *S-N* curves for the experimental fatigue test results

Case		*m*	$C_{ref,char}$ [10^]	$C_{ref,mean}$ [10^]	$FAT_{ref,char}$ [MPa]	$FAT_{ref,mean}$ [MPa]	1 : T_σ * [-]
Nykänen *et al.* [3, 4]: Skriko *et al.* [7]:		5.85	20.83	21.59	304	411	1.82
Case 1: r = 1 mm, d = 0, σ_{res} = measured	Standard, free *m*	3.73	16.12	16.47	428	531	1.54
	Standard, fixed *m*	4.00	16.92	17.27	452	554	1.50
	MSSPD	5.08	20.09	20.50	521	627	1.45
Case 2: $r = r_{true}$+1 mm, d = 0, σ_{res} = measured	Standard, free *m*	2.37	11.51	12.00	157	252	2.58
	Standard, fixed *m*	4.00	16.02	16.60	269	377	1.96
	MSSPD	4.83	18.27	18.95	301	417	1.92
Case 3: $r = r_{true}$+1 mm, d = 0, σ_{res} = -38 MPa	Standard, free *m*	3.57	15.05	15.46	280	366	1.71
	Standard, fixed *m*	4.00	16.26	16.68	308	392	1.62
	MSSPD	5.68	20.94	21.46	378	467	1.52
Case 4: $r = r_{true,average}$+1 mm, d = 0, σ_{res} = measured	Standard, free *m*	2.89	13.00	13.44	209	299	2.04
	Standard, fixed *m*	4.00	16.11	16.60	283	375	1.75
	MSSPD	5.02	18.91	19.49	324	422	1.70
Case 5: $r = r_{true,average}$+1 mm, d = 0, σ_{res} = -38 MPa	Standard, free *m*	4.17	16.77	17.13	326	399	1.50
	Standard, fixed *m*	4.00	16.30	16.66	316	390	1.53
	MSSPD	5.85	21.50	21.93	396	469	1.40

* The scatter range, P_s = 2.3%: P_s = 97.7%

The continuous *S-N* curves for the stress ratios R = 0.1–0.5 are presented in Figure 12. The stress ratio R = 0.25 (green) and 0.38 (blue) results follow the corresponding continuous *S-N* curves quite well but are slightly above the mean *S-N* curves. The high *R*-ratio results are clearly below the corresponding mean *S-N* curve but are barely above the characteristic *S-N* curve. The highest scatter is on the results of R = 0.1 and R = 0.5. The predicted *S-N* curves are almost straight lines in the log-log scale (Figure 12) when residual stresses are close to zero (assumed σ_{res} = -38 MPa). If the residual stresses were more compressive stresses, the shape of the curves would be more concave.

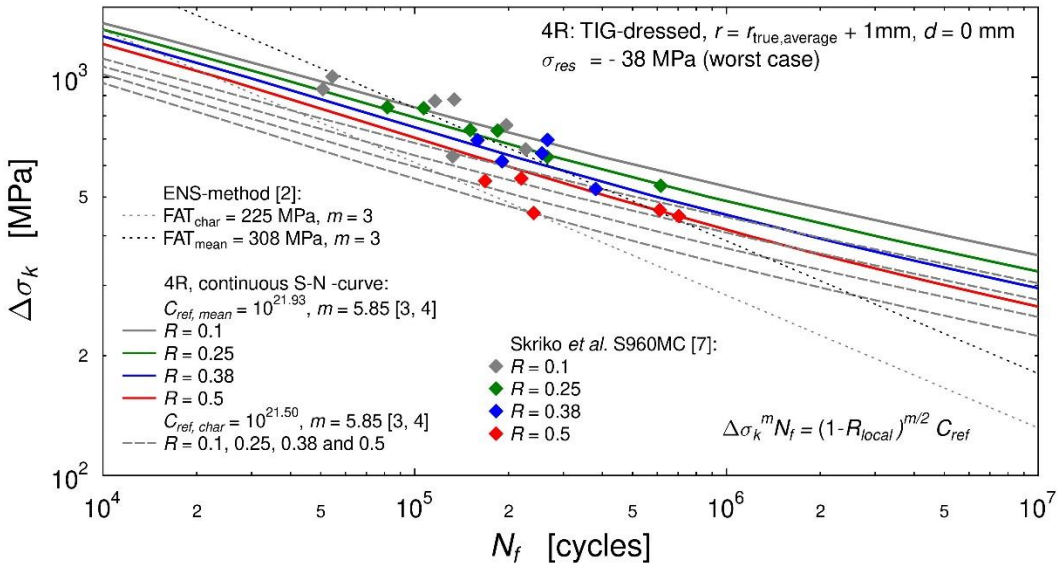

Figure 12. The continuous *S-N* curves for the 4R method using different stress ratio values R = 0.1–0.5. The averaged fictitious notch radius $r = r_{true,\ average}$ + 1 mm at the weld toe and the worst-case assumption for residual stresses σ_{res} = -38 MPa are used.

DISCUSSION

In the present study, the fatigue strength of UHSS fillet-welded joints post-weld treated with TIG-dressing was evaluated using conventional stress-based approaches, i.e. the nominal, structural hot spot and ENS methods, and a multi-parametric fatigue strength assessment approach known as the 4R method. The results showed that the fatigue strength prediction using the 4R method for TIG-dressed fillet welds is good. The conventional ENS method also matched quite well with the experimental results when $r = r_{true}$ + 1 mm was used. Figure 13 compares the experimental test results and calculated fatigue lives using the conventional methods (nominal stress, structural hot spot stress and ENS) and the 4R method, thereby showing that the 4R and ENS methods provide a good estimation of fatigue life for TIG-dressed cruciform joints. In Figure 8b, the experimental results and calculated *S-N* curve with the weld toe radius $r = r_{true}$ + 1 mm and the undercut d = 0 mm match quite well with FAT309 (mean value for the characteristic value FAT225).

Table 7 and Table 8 presented the scatter range for all applied methods with different cases (Nom, HS, ENS and 4R). Comparing the results and defined scatter range values, based on standard curve-fitting procedure with fixed slope m = 4 (slope is same in all cases, so results are comparable), it can be observed that in the 4R method case 5 ($r = r_{true,average}$ + 1 mm and σ_{res} = -38 MPa) the scatter range of T_σ = 1:1.53 is lowest and the *S-N*-curve is quite near to the master *S-N* curve. In the case 1 (4R), Table 8, the scatter range is small T_σ = 1:1.50, but the predicted *S-N* curve is above the master S-N curve. Thus, the used of fixed weld toe radius of r = 1 mm is not applicable in the 4R (or ENS) method.

Yildirim *et al*. [11] proposed the use of r = 1 mm for HFMI-treated welds. They concluded that fatigue strength improvement using HFMI treatment is generally dependent on the induced compressive residual stress rather than on the enhanced shape of the weld toe rounding. In TIG-dressed weld joints, the induced compressive residual stress state is lower than in HFMI-treated joints, but the radii of the weld toes are significantly larger. Based on the results of this study, the use of the toe radii $r = r_{true} + 1$ mm for TIG-dressed cruciform joints can be proposed. Stress gradient effects at notched members could potentially be addressed more comprehensively using the stress averaging and critical distance concepts [18,35], but their applications lie beyond the scope of the present study.

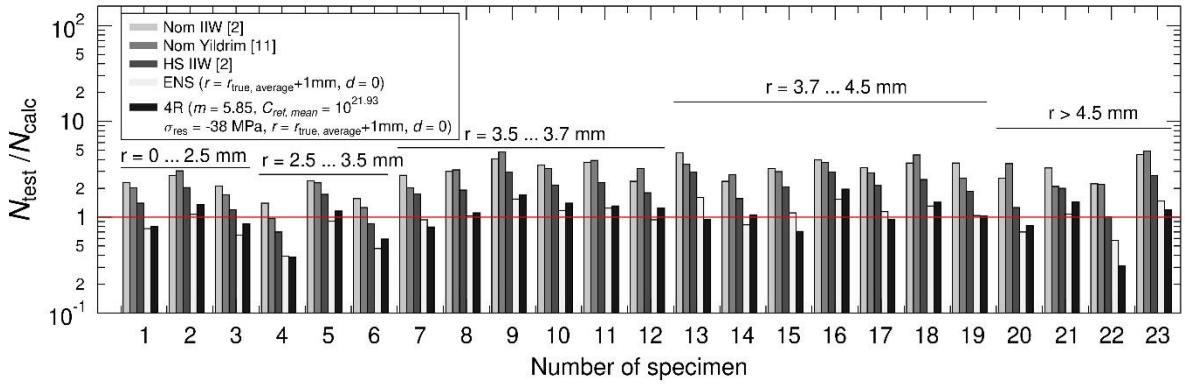

Figure 13. Comparison of the experimental fatigue test results based on the 4R and conventional fatigue assessment methods.

The regression analysis showed that the slope of the *S-N* curve was higher than m = 3 for TIG-dressed joints. The slope was m = 3.5 using the MSSPD curve-fitting procedure for the nominal stress method and m = 3.3–3.4 for the hot spot and ENS methods. In the 4R method, the calculated slope of the reference *S-N* curve for all test specimens was m = 4.8–5.8 using the MSSPD curve-fitting method. Yildirim *et al.* [11] and Bousseau and Millot [36] also presented matching results regarding the slope of the *S-N* curve for joints in the TIG-dressed condition.

Defining a correct residual stress level corresponding to the failure location is problematic because crack initiation can occur, for instance, at the middle of the TIG-dressed area or at the fusion line of the TIG-dressing. In this study, the residual stresses after TIG-dressing were determined on the boundary between the TIG-dressed zone and the base material (base material side). The location of the measurement point and the place of crack initiation are not the same in the test specimens and, consequently, the maximum value of the residual stress measurements (-38 MPa) was assumed to represent the residual stress level in each test specimen. The characterized residual stress seems to give a good correspondence between the experiments and the 4R analysis.

Figure 14 presents all the residual stress measurements after TIG-dressing. The residual stresses on the surface after TIG-dressing are quite variable. The measured compressive residual stresses were between -38 and -480 MPa, although one of the test specimens had a tension residual stress of 250 MPa. The average of the measured residual stresses is -188 MPa if all specimens are taken into account, and -242 MPa if one measured tensile residual stress value, equal to σ_{res} = 250 MPa, is left out as an outlier. The "worst" residual stress level at the weld toe after TIG-dressing is simply approximated based on the measurements and a value of σ_{res} = -38 MPa is assumed to represent all TIG-dressed test specimens in this study.

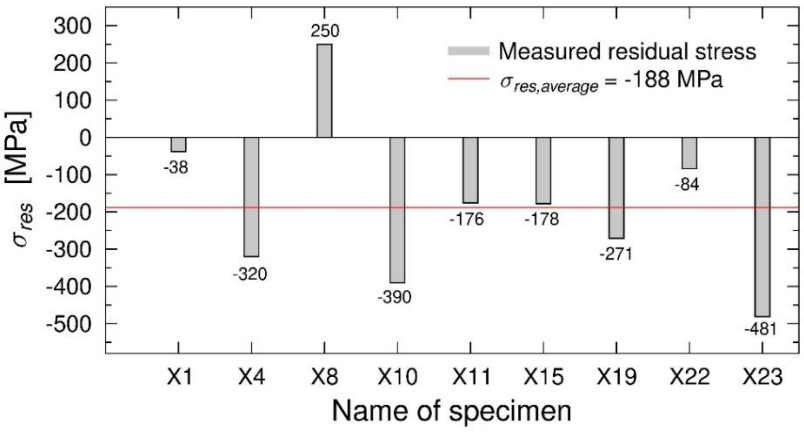

Figure 14. Measured residual stresses parallel to the loading direction in the weld toes of cruciform joints after TIG-dressing.

The material model in the 4R method is based on the R-O material model with the parameters of Young's modulus *E*, strength coefficient *H*, and elastic-plastic strain hardening exponent *n* (Equations 1 and 3). The effect of microstructural hardening or softening caused by TIG-dressing can be taken into account by means of modifying the R-O material parameters. The remelting of the weld and base material caused a new fusion and HAZs, which had different material properties than the base material. Hardness measurements showed softening in the HAZ and the fusion line of the TIG-dressing (Figure 5). Fatigue strength prediction can be expected to be more accurate if a specific stress-strain curve is utilized for weld and HAZ material after TIG-dressing. In addition, the material properties relative to the location of the crack initiation play a significant role. By gaining a closer insight into the material parameters and residual stresses specific to the actual failure location, the accuracy of the 4R fatigue strength prediction are expected to be improved. In the present study, the material parameters and residual stresses were characterized for the whole fatigue test series as extensive measurements of these values were not available. Furthermore, the present study analyzed small-scale specimens with relatively low residual stresses and the fatigue behavior of fillet-welded and TIG-dressed joints was mainly controlled by the weld toe radius. Hence, the ENS method also gave accurate results for the applied fatigue test data. Nevertheless, in the 4R method, the essential parameters affecting the fatigue behavior of welded joints can be implemented in the fatigue analysis.

CONCLUSIONS

This study applied a novel multi-parametric fatigue design approach, the 4R method, to predict the fatigue strength of TIG-dressed UHSS fillet weld joints under CA tensile loading in a series of experimental fatigue tests. Only joints with weld toe failures were investigated. In addition, conventional stress-based approaches, namely the nominal, structural stress and ENS methods, were also used. The experimental fatigue data of TIG-dressed weld joints from the literature were also analyzed in a reference coordinate system.

The main focus of this study was to show the applicability the 4R method for predicting fatigue strength, and to investigate if the master *S-N* curve is also suitable for TIG-dressed UHSS fillet weld joints. The 4R parameters must be known, measured or estimated appropriately, representative of the worst-case conditions of a welded joint, to convert data into the reference system. Based on the experimental measurements, fatigue test results and calculations, the following conclusions can be drawn:

- In general, TIG-dressing had a beneficial effect on the geometry of the weld toe but, due to a manually performed treatment, there was more quality variation regarding the weld toe radius after TIG-dressing compared to in a mechanically or robotically conducted ASW condition.
- The recommended design *S-N* curves of the nominal stress and structural stress methods [2,11] were conservative for TIG-dressed fillet weld joints.
- The use of a fictitious notch radius r = 1 mm is not reasonable for the FE analysis of TIG-dressed weld joints because the radius of the toe rounding is notably larger after remelting and this causes a lower stress concentration factor K_t.
- The 4R method is suitable fatigue life assessment method for consideration the essential parameters affecting the fatigue performance of the TIG-dressed joints
- In the 4R method, the averaged fictitious notch radius $r = r_{\text{true, average}} + 1$ mm at the weld toe for TIG-dressed weld joints showed good correspondence between the experimental results and fatigue life estimation.
- The predicted worst-case residual stress assumption for TIG-dressing provided results that are above the characteristic master *S-N* curve. The prediction results are on the safe side.
- Analyzing fatigue test results with a radius of $r = r_{\text{true}} + 1$ mm at the weld toe and using the ENS method showed a good correspondence with the FAT225 *S-N* curve.

ACKNOWLEDGEMENTS

The research was funded by the Business Finland.

REFERENCES

[1] EN 1993-1-9. Eurocode 3 - Design of steel structures - Part 1-9: Fatigue 2005.

[2] Hobbacher AF. Recommendations for Fatigue Design of Welded Joints and Components. Springer International Publishing; 2016.

[3] Nykänen T, Björk T. Assessment of fatigue strength of steel butt-welded joints in as-welded condition - Alternative approaches for curve fitting and mean stress effect analysis. Mar Struct 2015;44:288–310. https://doi.org/10.1016/j.marstruc.2015.09.005.

[4] Nykänen T, Björk T. A new proposal for assessment of the fatigue strength of steel butt-welded joints improved by peening (HFMI) under constant amplitude tensile loading. Fatigue Fract Eng Mater Struct 2016;39:566–82. https://doi.org/10.1111/ffe.12377.

[5] Björk T, Mettänen H, Ahola A, Lindgren M, Terva J. Fatigue strength assessment of duplex and super-duplex stainless steels by 4R method. Weld World 2018;62:1285–300. https://doi.org/10.1007/s40194-018-0657-8.

[6] Ahola A, Skriko T, Björk T. Fatigue strength assessment of ultra-high-strength fillet weld joints using 4R method (in press). J Constr Steel Res 2019. https://doi.org/10.1016/j.jcsr.2019.105861.

[7] Skriko T, Ghafouri M, Björk T. Fatigue strength of TIG-dressed ultra-high-strength steel fillet weld joints at high stress ratio. Int J Fatigue 2017;94:110–20. https://doi.org/10.1016/j.ijfatigue.2016.09.018.

[8] Hensel J, Nitschke-pagel T, Dilger K. Fatigue performance of welded steel longitudinal stiffeners. ISOPE 2012, International Society of Offshore and Polar Engineers; 2012.

[9] Hensel J, Nitschke-pagel T, Schönborn S, Dilger K. Factors affecting the knee point position of S-N curves of welds with longitudinal stiffeners. IIW Doc XIII-2441-12 2012.

[10] Haagensen PJ, Maddox SJ. IIW Recommendations on Post Weld Fatigue Life Improvement of Steel and Aluminium Structures. IIW Doc XIII-2200r7-07 2010.

[11] Yildirim HC. Review of fatigue data for welds improved by tungsten inert gas dressing. Int J Fatigue 2015;79:36–45. https://doi.org/10.1016/j.ijfatigue.2015.04.017.

[12] Dahle T. Design fatigue strength of TIG-dressed welded joints in high-strength steels subjected to spectrum loading. Int J Fatigue 1998;20:677–81.

[13] Huo L, Wang D, Zhang Y. Investigation of the fatigue behaviour of the welded joints treated by TIG dressing and ultrasonic peening under variable-amplitude load. Int J Fatigue 2005;27:95–101. https://doi.org/10.1016/j.ijfatigue.2004.05.009.

[14] Kirkhope KJ, Bell R, Caron L, Basu RI, Ma K. Weld detail fatigue life improvement techniques. Part 2: application to ship structures. Mar Struct 1999;12:477–96.

[15] Pedersen MM, Mouritsen OØ, Hansen MR, Andersen JG, Wenderby J. Comparison of post-weld treatment of high-strength steel welded joints in medium cycle fatigue. Weld World 2010;54:208–17.

[16] Ramalho AL, Ferreira JAM, Branco CAGM. Fatigue behaviour of T welded joints rehabilitated by tungsten inert gas and plasma dressing. Mater Des 2011;32:4705–13. https://doi.org/10.1016/j.matdes.2011.06.051.

[17] Rudolph J, Schmitt C, Wei E. Fatigue lifetime assessment procedures for welded pressure vessel components. Int J Press Vessel Pip 2002;79:103–12.

[18] Baumgartner J, Yildirim HC, Barsoum Z. Fatigue strength assessment of TIG-dressed welded steel joints by local approaches 2019;126:72–8. https://doi.org/10.1016/j.ijfatigue.2019.04.038.

[19] Björk T, Ahola A, Skriko T. 4R method for consideration of the fatigue performance of welded joints - Background and applications. In: Chan S-L, Chan T-M, Zhu S, editors. Ninth Int. Conf. Adv. Steel Struct. (ICASS 2018), Hong Kong: 2018, p. 1159–68. https://doi.org/10.18057/ICASS2018.xxx.

[20] Ahola A, Skriko T, Björk T. Experimental investigation on the fatigue strength assessment of welded joints made of S1100 ultra-high-strength steel in as-welded and post-weld treated condition. In: Zingoni A, editor. Proc. 7th Int. Conf. Struct. Eng. Mech. Comput. (SEMC 2019). Cape Town, South Africa, 2-4 Sept. 2019, 2019, p. 1254–9.

[21] Nykänen T, Mettänen H, Björk T, Ahola A. Fatigue assessment of welded joints under variable amplitude loading using a novel notch stress approach. Int J Fatigue 2017;101:177–91. https://doi.org/10.1016/j.ijfatigue.2016.12.031.

[22] Radaj D, Sonsino M, Fricke W. Fatigue assessment of welded joints by local approaches, 2nd ed. Cambridge: Woodhead Publishing; 2006.

[23] Nykänen T, Björk T, Laitinen R. Fatigue strength prediction of ultra high strength steel butt-welded joints. Fatigue Fract Eng Mater Struct 2012;36:469–82. https://doi.org/10.1111/ffe.12015.

[24] Ahola A, Skriko T. 4R method for consideration of the fatigue performance of welded joints - Background and applications. Chan S-L, Chan T-M, Zhu S Ninth Int Conf Adv Steel Struct (ICASS 2018) Hong Kong 2018:5–7. https://doi.org/10.18057/ICASS2018.xxx.

[25] Karakas Ö. Consideration of mean-stress effects on fatigue life of welded magnesium joints by the application of the Smith-Watson-Topper and reference radius concepts. Int J Fatigue 2013;49:1–17. https://doi.org/10.1016/j.ijfatigue.2012.11.007.

[26] WE D. Statistical adjustment of data. NY (Dover Publications Edition, 1985): Wiley; 1943.

[27] Tateishi K, Hanji T, Hanibuchi S. Improvement of extremely low cycle fatigue strength of welded joints by toe finishing. Weld World 2009;53:238–45.

[28] Sonsino CM, Fricke W, Bruyne F De, Hoppe A, Ahmadi A, Zhang G. Notch stress concepts for the fatigue assessment of welded joints – Background and applications. Int J Fatigue 2012;34:2–16. https://doi.org/10.1016/j.ijfatigue.2010.04.011.

[29] Karakas Ö, Morgenstern C, Sonsino CM. Fatigue design of welded joints from the wrought magnesium alloy AZ31 by the local stress concept with the fictitious notch radii of r_f = 1.0 and

0.05 mm. Int J Fatigue 2008;30:2210–9. https://doi.org/10.1016/j.ijfatigue.2008.05.017.

[30] Karakas Ö. Application of Neuber's effective stress method for the evaluation of the fatigue behaviour of magnesium welds. Int J Fatigue 2017;101:115–26. https://doi.org/10.1016/j.ijfatigue.2016.10.023.

[31] Baumgartner J. Review and considerations on the fatigue assessment of welded joints using reference radii. Int J Fatigue 2017;101:459–68. https://doi.org/10.1016/j.ijfatigue.2017.01.013.

[32] Fricke W. Guideline for the Fatigue Assessment by Notch Stress Analysis for Welded Structures. IIW Doc XIII-2240r2-08/XV-1289r2-08 2010.

[33] Baumgartner J, Bruder T. An efficient meshing approach for the calculation of notch stresses. Weld World 2013:137–45. https://doi.org/10.1007/s40194-012-0005-3.

[34] Sonsino CM, Bruder T, Baumgartner J. S-N lines for welded thin joints -Suggested slopes and FAT values for applying the notch stress concept with various reference radii. Weld World 2010;54:375–92.

[35] Karaka Ö, Zhang G, Sonsino CM. Critical distance approach for the fatigue strength assessment of magnesium welded joints in contrast to Neuber's effective stress method. Int J Fatigue 2018;112:21–35. https://doi.org/10.1016/j.ijfatigue.2018.03.004.

[36] Bousseau M, Millot T. Fatigue life improvement ofwelded structures by ultrasonic needle peening compared to tig dressing. IIW Doc. XIII-2125-06, 2006.